

Figure 1: Micrograph showing the microstructure of AD995 alumina. Sample was thermally etched in air at 1550°C for 30 minutes to reveal grain boundaries.

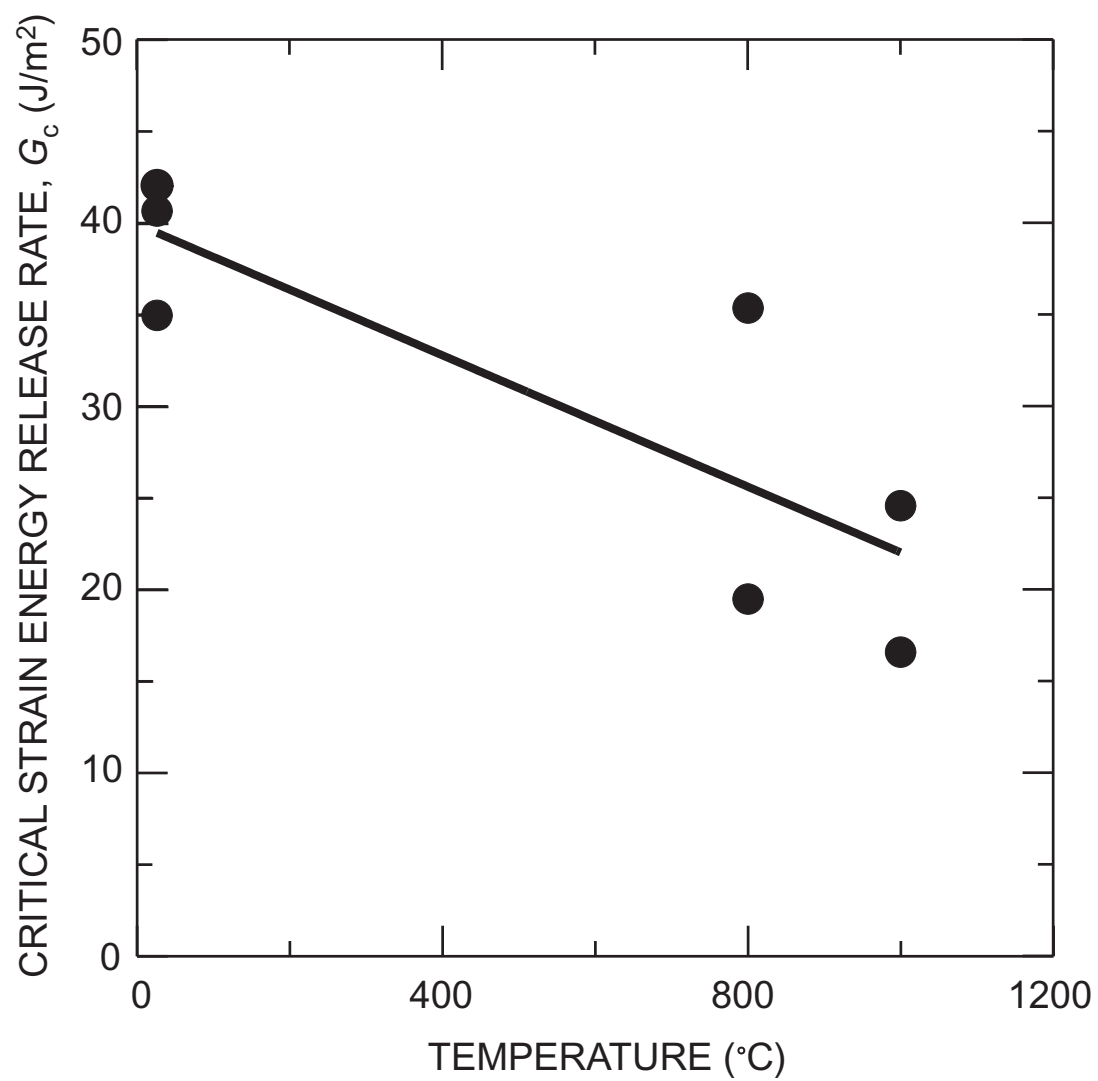


Figure 2: Interfacial fracture toughness of PTLP bonded joints as a function of temperature. Elevated temperature tests were performed in gettered argon.

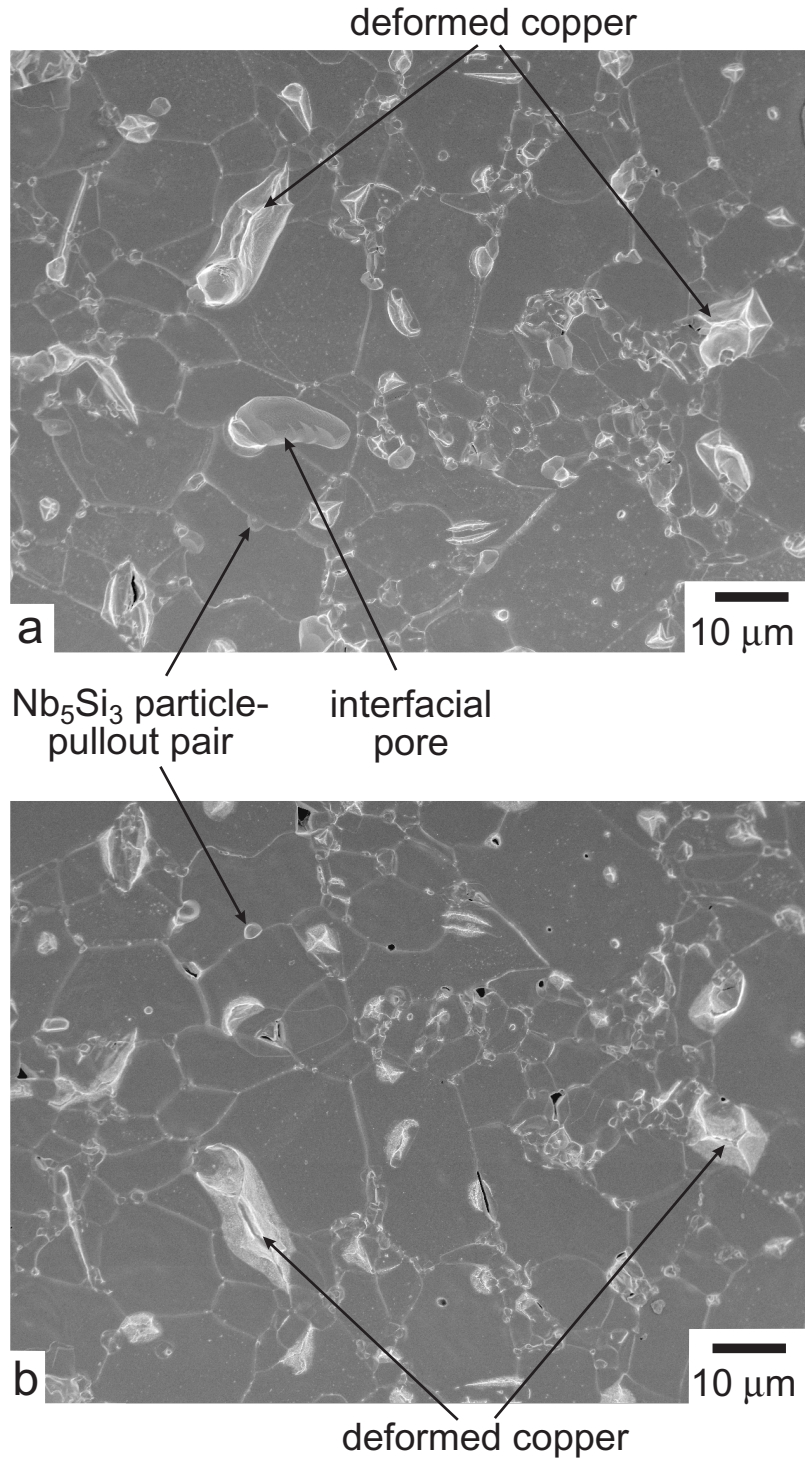


Figure 3: Matching micrographs of the same region of the (a) niobium and (b) alumina side of the fast fracture surfaces. The deformed copper regions are adhered to both sides of the fracture surface while  $\text{Nb}_5\text{Si}_3$  particles are only on alumina side. Grain boundary grooving is evident in the alumina, with matching imprints appearing in the niobium. Direction of crack propagation was left to right with respect to the micrograph.

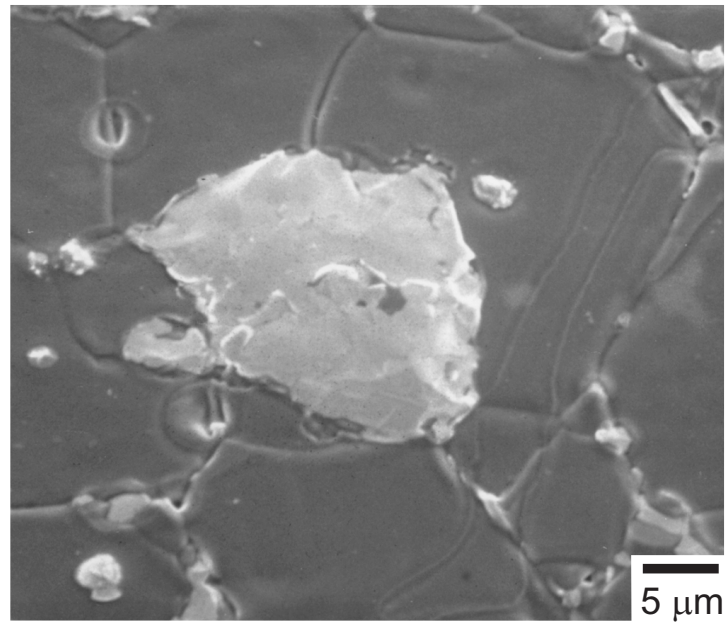


Figure 4: Micrograph of a large Nb<sub>5</sub>Si<sub>3</sub> particle on the alumina side of the fast fracture surface that was used for quantitative EDS measurements. Direction of crack propagation was left to right with respect to the micrograph.



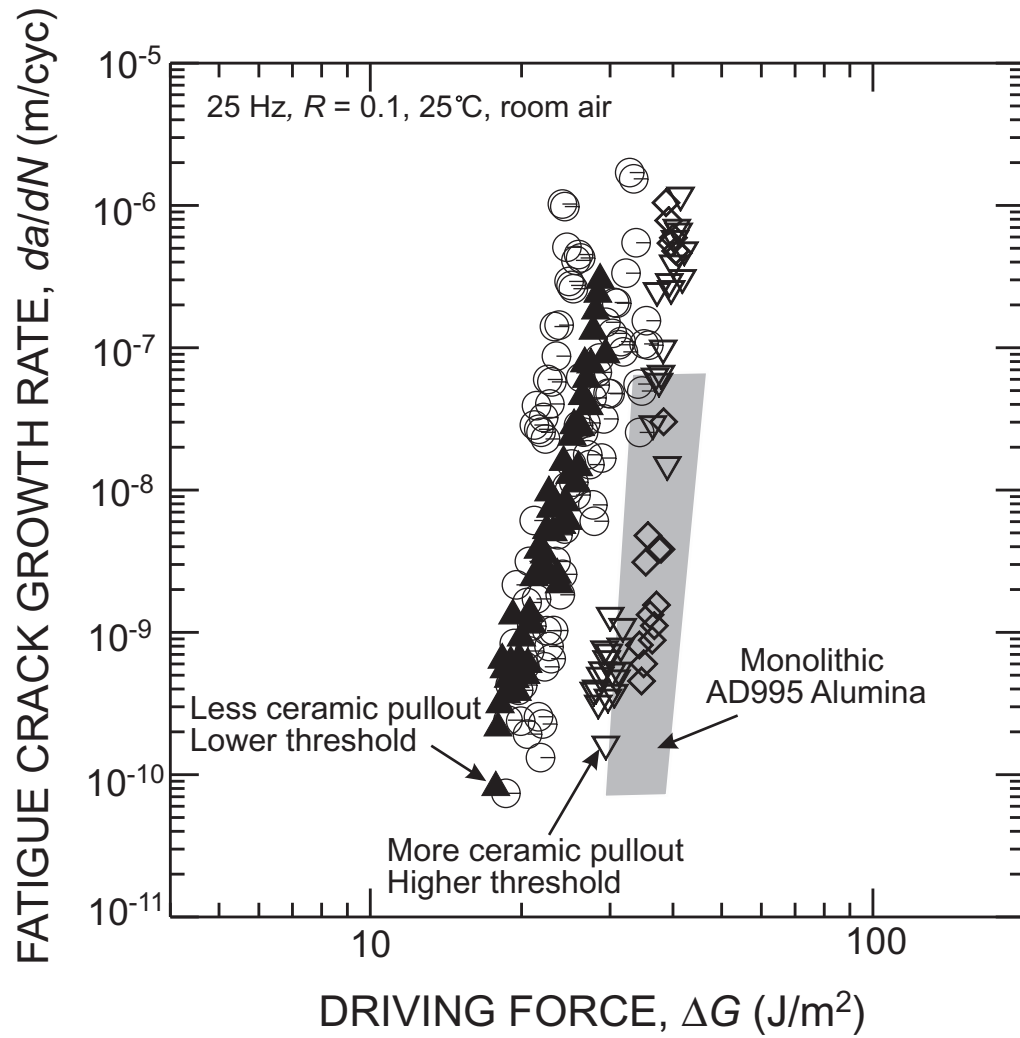


Figure 5: Fatigue-crack growth rates for PTLP bonded sandwich specimens. Individual symbols correspond to different individual samples. Higher fatigue thresholds were measured for samples with more alumina grain pullout during fatigue-crack growth.

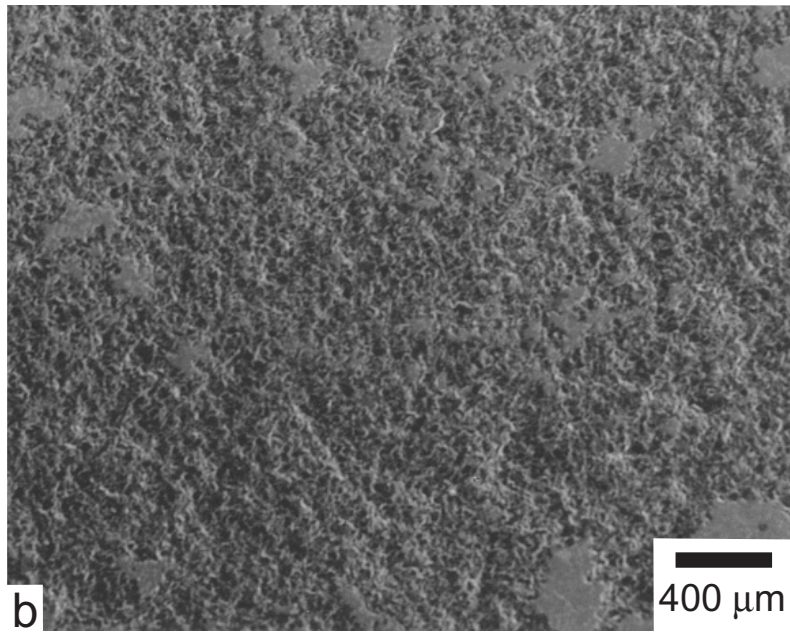
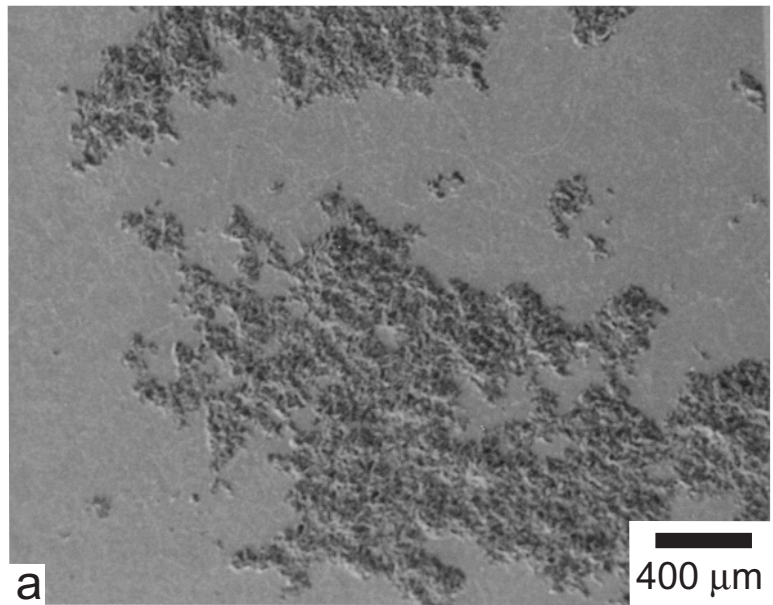


Figure 6: Micrographs of fatigue fracture surfaces showing (a)  $\sim 50\%$  and (b)  $\sim 100\%$  alumina grain pullout. For the latter case, fatigue-crack propagation was almost entirely in the alumina. Direction of crack propagation was left to right with respect to the micrograph.

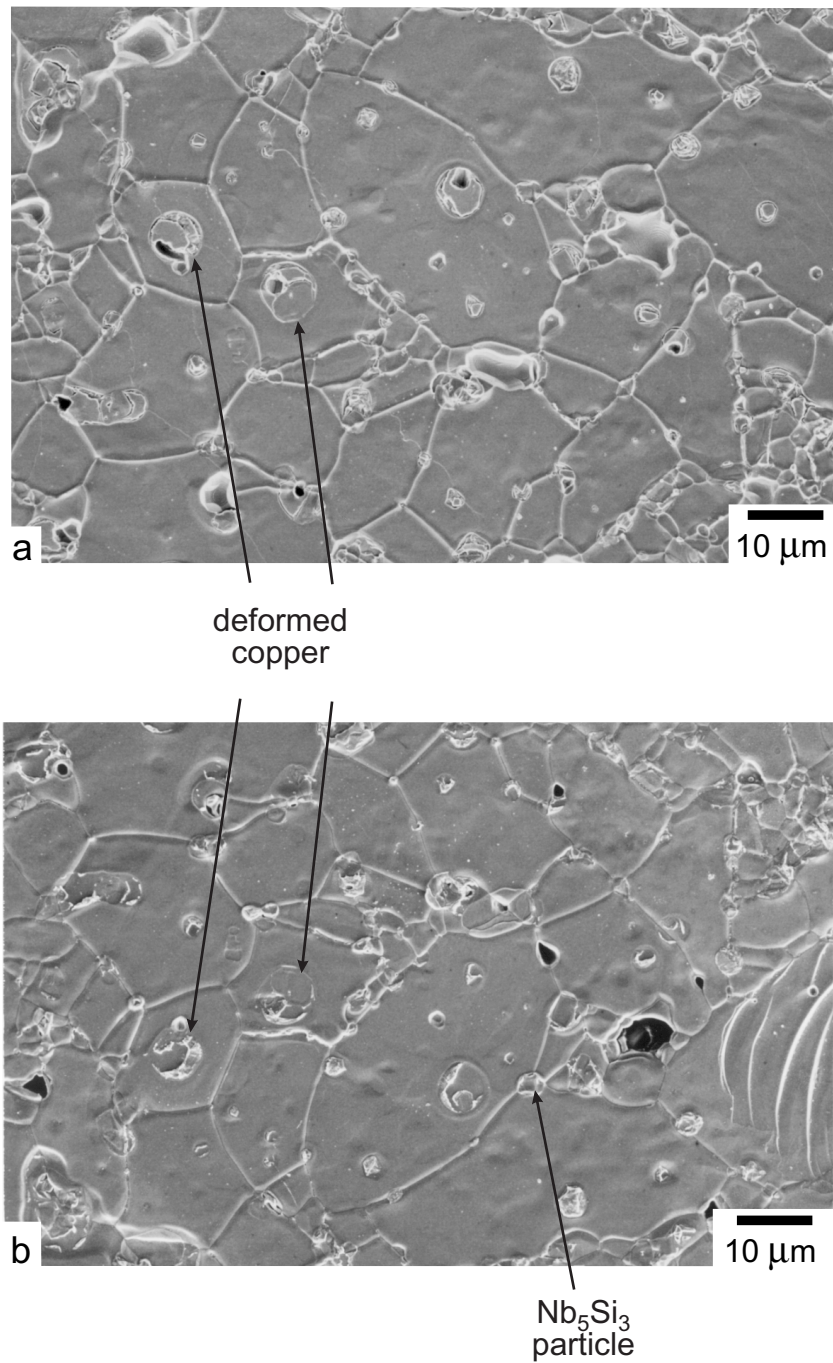


Figure 7: Matching micrographs of the same region of the (a) niobium and (b) alumina side of the fatigue fracture surfaces. Deformed copper regions appear flattened with some separation of the alumina/copper interface visible. Matching imprints of the alumina grain boundaries can be seen in the niobium. Direction of crack propagation was left to right with respect to the micrograph.

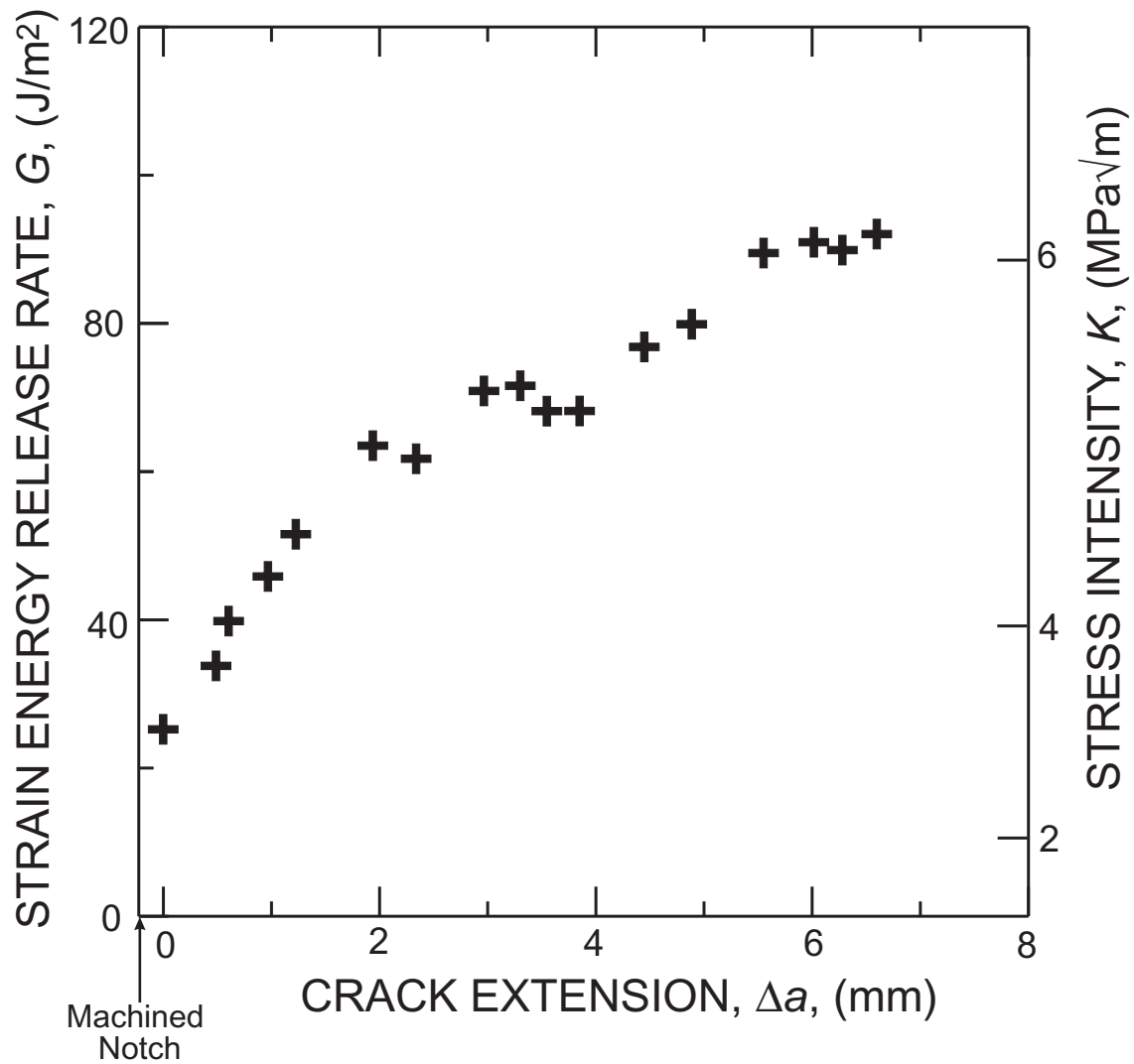


Figure 8: R-curve measured for Coors AD995 alumina demonstrating rising crack-growth resistance with crack extension. Data shown were collected from a fatigue pre-cracked C(T) sample where the pre-crack was grown only 230  $\mu\text{m}$  from the machined notch to minimize the initial crack length.

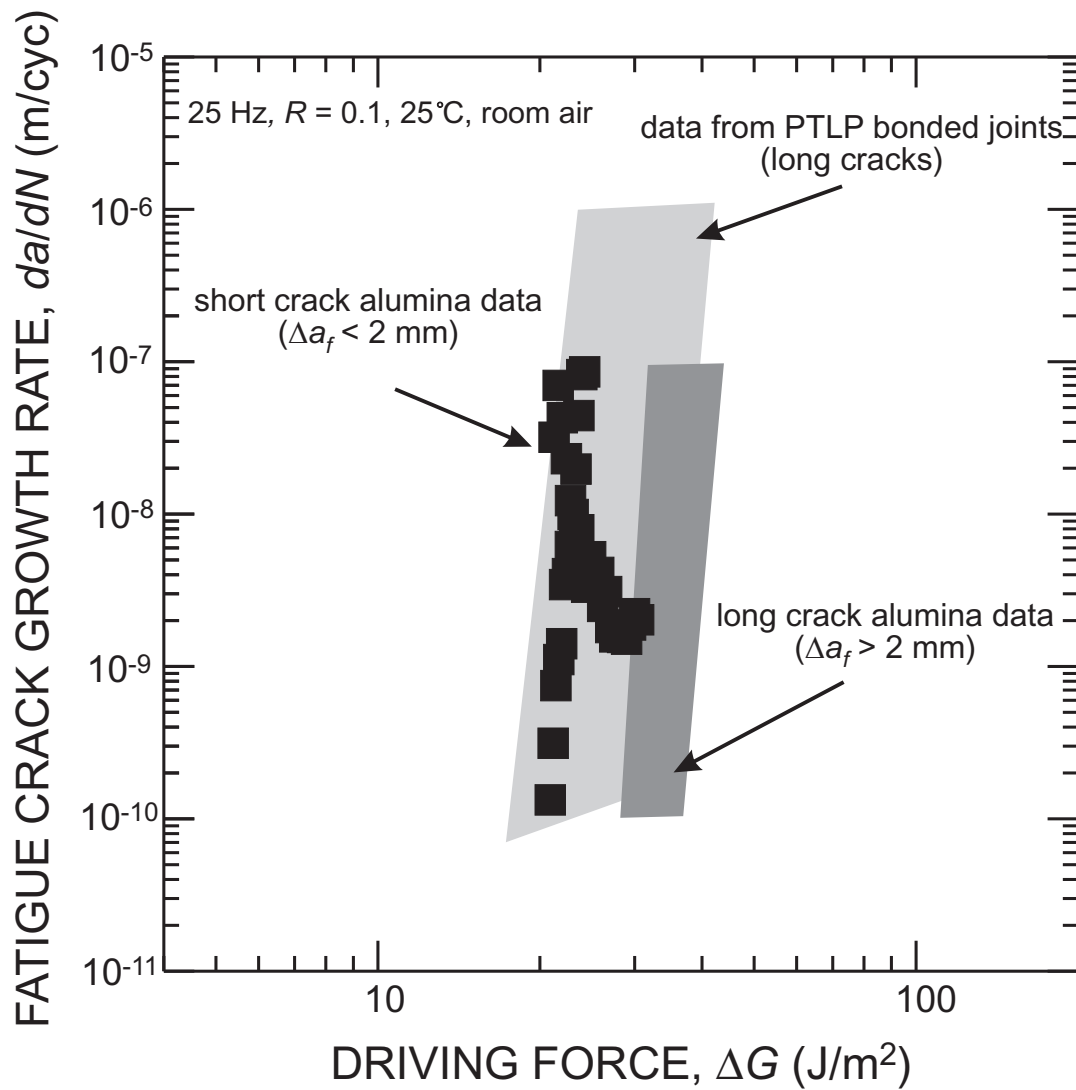


Figure 9: Fatigue-crack growth rates for short ( $\Delta a_f < 2$  mm) fatigue cracks in Coors AD995 alumina where grain bridging was limited due to the short wake behind the crack tip. Note that the short crack data compare favorably with the data for PTLP joints where alumina grain bridging was limited due to a partial ( $\sim 50\%$ ) interfacial crack path.